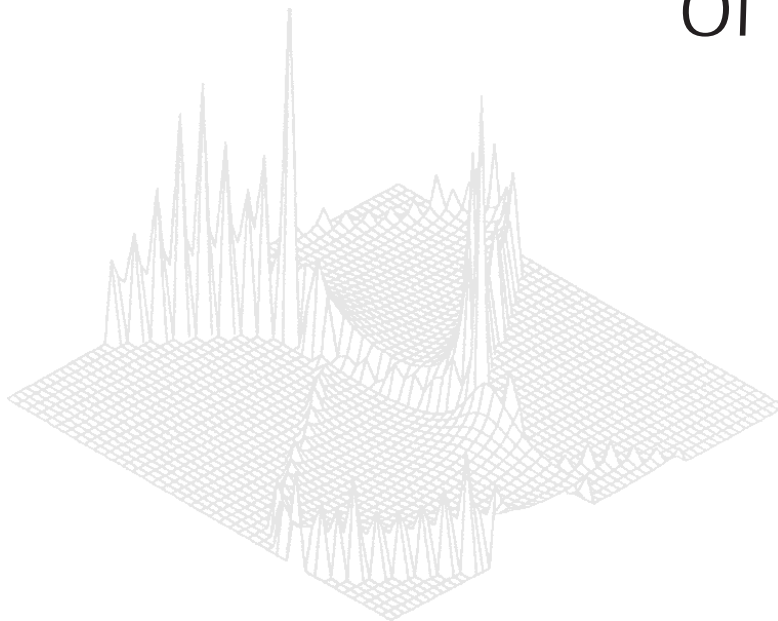

C S I R O P U B L I S H I N G

Australian Journal of Physics

Volume 51, 1998
© CSIRO 1998



A journal for the publication of
original research in all branches of physics

www.publish.csiro.au/journals/ajp

All enquiries and manuscripts should be directed to

Australian Journal of Physics

CSIRO PUBLISHING

PO Box 1139 (150 Oxford St)

Collingwood

Vic. 3066

Australia

Telephone: 61 3 9662 7626

Facsimile: 61 3 9662 7611

Email: peter.robertson@publish.csiro.au



Published by **CSIRO PUBLISHING**
for CSIRO and the
Australian Academy of Science



Magnetic Behaviour of Systems with a Quasi-doublet Ground State*

P. C. M. Gubbens and A. M. Mulders

Interfacultair Reactor Instituut, TUDelft,
2629 JB Delft, The Netherlands.

Abstract

In this paper we will present a study of several Tm and Pr compounds, where the rare earth atoms have as their two lowest energy levels a quasi-doublet ground state. These compounds are also compared with Er and/or Dy compounds, which have a Kramers doublet as ground state. Four compounds (TmNi₅, TmCu₂, TmCuAl and PrRu₂Si₂) are discussed in sequence, where the energy separation of the two levels of the quasi-doublet ground state doublet is increasing. These compounds were studied with rare earth Mössbauer spectroscopy and μ SR as the main measuring techniques.

1. Introduction

In intermetallic compounds of Tm and Pr, the trivalent rare earth atoms are non-Kramers atoms with an integer angular momentum quantum number ($J = 6$ and 4 for Tm and Pr respectively). For hexagonal local symmetry (or lower), the electronic ground state of these atoms often consists of a pair of non-degenerate, non-magnetic singlets. Nevertheless, a very large cross term between the two singlets can lead to magnetism with an easy direction of magnetisation parallel to the c axis. Therefore, the two singlets can be regarded as a quasi-doublet. This behaviour is in contrast with Kramers doublets of Dy and Er ($J = \frac{15}{2}$), which are already magnetic and whose degeneracy is lifted only by the magnetic interaction.

In this paper we consider results accumulated over the last twelve years for several Tm and Pr intermetallic compounds and compare them with results for isostructural compounds of Er. The results will be presented in the sequence of increasing energy separation of the quasi-doublet ground-state levels. First, results for ErNi₅ ($T_C = 9.2$ K) and TmNi₅ ($T_C = 4.5$ K) show that the dynamic fluctuations of the magnetic spins above T_C are comparably slow compared with the nuclear Larmor precession frequency (Gubbens *et al.* 1985, 1989). In the case of TmNi₅ the splitting between the two levels of the quasi-doublet ground state is only 0.4 K as determined recently by Kayzel (1997). For TmNi₅, the temperature dependence of the magnetic relaxation above T_C shows an exponential behaviour.

* Refereed paper based on a contribution to the International Workshop on Nuclear Methods in Magnetism, held in Canberra on 21–23 July 1997.

Secondly, the relaxation behaviour of the orthorhombic compounds ErCu_2 ($T_N = 11.5$ K) and TmCu_2 ($T_N = 6.3$ K) will be discussed (Gubbens *et al.* 1991, 1992*b*). For TmCu_2 the temperature dependence of the magnetic relaxation between the two energy levels with a splitting of about 1 K still has an exponential behaviour (Gubbens *et al.* 1992).

Furthermore, ^{169}Tm Mössbauer measurements of the hexagonal compound TmCuAl ($T_N = 1.86$ K) will be discussed. From a study of the pseudo-quadrupolar shift and the relaxation behaviour we found an energy splitting of 2 K (Gubbens *et al.* 1998).

Finally, we will show results for the tetragonal compound PrRu_2Si_2 . This compound undergoes a magnetic phase transition to an axial incommensurate structure at $T_N \sim 16$ K, followed by a first order phase transition to an axial ferromagnet at $T_C \sim 14$ K. In this case the two lowest energy levels are separated by 25 K (Mulders *et al.* 1997).

All these compounds were studied by rare earth Mössbauer spectroscopy. The RNi_5 and PrRu_2Si_2 compounds were studied by μSR . Additive neutron and solid measuring techniques were also used in most cases.

2. Theoretical Aspects

The crystal field acting at a trivalent rare earth atom can be described by means of a Hamiltonian, which is for hexagonal local symmetry

$$H_c = B_2^0 O_2^0 + B_4^0 O_4^0 + B_6^0 O_6^0 + B_6^6 O_6^6, \quad (1)$$

and for tetragonal local symmetry

$$H_c = B_2^0 O_2^0 + B_4^0 O_4^0 + B_4^4 O_4^4 + B_6^0 O_6^0 + B_6^4 O_6^4. \quad (2)$$

In these formula O_n^m are operator equivalents and $B_n^m = \theta_n \langle r^n \rangle A_n^m$. Here θ_n represents the Stevens constants α_J , β_J and γ_J for $n = 2, 4$ and 6 , respectively. The symbol $\langle r^n \rangle$ represents Hartree–Fock radial averages and A_n^m are the crystal field potentials. For lower symmetry, e.g. orthorhombic, one had to include all even terms in the crystal field Hamiltonian and the number of crystal fields increases to nine.

When we include the interaction of the rare earth moments with the molecular field H_M present at these sites, the Hamiltonian H becomes

$$H = H_c - g_J \mu_B H_M J_z. \quad (3)$$

In this expression the quantity g_J is the Landé g factor. The energy levels with their corresponding eigenfunctions can be determined after diagonalisation of the Hamiltonian.

Generally, in rare earths with an integer value of J as Pr and Tm with $B_2^0 < 0$ (with a c axis magnetic anisotropy) the two lowest levels of the crystal field scheme are

$$\sqrt{\frac{1}{2}}(|+J\rangle - |-J\rangle) \quad (4)$$

as first excited state and

$$\sqrt{\frac{1}{2}}(|+J\rangle + |-J\rangle + \delta|0\rangle) \quad (5)$$

as ground state for a site with a local hexagonal symmetry. Space group codes for these two levels are $|\Gamma_{t1}^{(1)}\rangle$ for the ground state and $|\Gamma_{t2}\rangle$ for the first excited state. In a symmetry lower than hexagonal more mixing is present with contributions from m_J values other than $|J\rangle = 4$ or 6 . In principle, each value of such a quasi-doublet is non-magnetic. However, the very large cross term between the two levels can lead to magnetism with an easy direction of magnetisation along the c axis.

3. Rare Earth Mössbauer Spectroscopy

In the case of rare earth Mössbauer spectroscopy the two important parameters are the magnetic hyperfine field (H_{eff}) and the electric quadrupole splitting (QS). The temperature dependence of these quantities is determined by the energies and the eigenfunctions of the crystal field levels of the rare earth ions via the expressions

$$H_{eff}(T) = H_{eff}^{4f}(0) \langle J_z \rangle_{av} / J, \quad (6)$$

$$QS(T) = QS^{4f}(0) \frac{\langle 3J_z^2 - J(J+1) \rangle_{av}}{J(2J-1)} + QS^{latt}, \quad (7)$$

where $\langle \rangle_{av}$ indicates a thermal average over the energy levels of the crystal field scheme, QS^{latt} is the lattice contribution of the electric quadrupole splitting, and $H_{eff}^{4f}(0)$ and $QS^{4f}(0)$ are the free ion values for the rare earths used at $T = 0$ K.

4. μ^+ SR Spectroscopy

The positive muon μ^+ is a point-like particle (lepton) with a positive elementary electric charge and a mass of about $\frac{1}{9}$ of the proton mass. These two properties explain the experimental fact that the muon can diffuse between interstitial sites in a crystal. The μ^+ diffusion may introduce experimental difficulties in studies of magnetic properties of compounds. However, at low temperatures the muon will be localised on one site. The μ^+ is a radioactive particle with a lifetime of $\tau_\mu = 2.2 \times 10^{-6}$ s and a spin $\frac{1}{2}$. It has a gyromagnetic ratio $\gamma_\mu = 8.52 \times 10^8$ rad s^{-1} and decays in the following way: $\mu^+ \rightarrow e^+ + \nu_e + \nu_\mu$. In the experiment only the positron e^+ will be detected. Its probability of emission is highly anisotropic [like $1 + A \cos(\theta)$], where θ is the angle between the direction of the muon spin at the time of its decay and the direction of emission of the positron. The parameter A depends on the positron energy and its average over all the possible positron energies is $\frac{1}{3}$. In practice A falls between 0.20 and 0.24. This factor is non-zero, because the μ^+ decay is a weak interaction process, which does not conserve parity. The μ^+ SR technique is based on two different experimental facts.

Firstly, a muon is produced with its polarisation antiparallel to its momentum so that it is naturally polarised. Secondly, the muon decay is anisotropic and its anisotropy is directly related to the μ^+ spin direction as mentioned above. Therefore, it is possible to follow the evolution of muon spin in a sample. The μ^+ SR technique is a time differential method. When a muon is implanted in a sample, a clock is started. This clock is stopped when its positron escapes from the sample. In an experiment, a histogram of the number of detected positrons versus the time given by the clock is measured.

The muon spin interacts with a magnetic field. Two experimental geometries can be used. They are referred to as the longitudinal and transverse field geometries, depending on whether the applied field is parallel or perpendicular to the initial beam polarisation. The number of positrons recorded can be represented by

$$N(t) = N_0 e^{-t/\tau_\mu} [1 + P(t) A \cos(\omega t)]. \quad (8)$$

Here A is the initial asymmetry and $P(t)$ is the μ^+ SR depolarisation function. The exponential decay function describes the fact that the muon has a lifetime of $2.2 \mu\text{s}$. In the transverse mode one measures the frequency

$$\omega = \gamma_\mu B_\mu$$

in which B_μ is the local field at the muon site. This field is due to two contributions. The dominant contribution is produced by the classical dipolar interaction between the localised electronic dipole moments and the μ^+ spin. The second contribution is produced by the conduction electrons at the muon site through the Fermi contact interaction. An important difference between μ^+ SR and other local probe techniques such as nuclear magnetic resonance (NMR), Mössbauer effect and perturbed angular correlation (PAC) is that B_μ is mainly determined by the dipolar interaction, whereas in the other techniques the contact interaction dominates.

Due to fluctuations of the local magnetic field, the μ^+ SR depolarisation function $P(t)$ will decrease with time. The exponential damping λ can be represented as

$$P(t) = e^{-\lambda t}, \quad (10)$$

with

$$\lambda = \gamma_\mu^2 \langle \Delta^2 \rangle \tau_c. \quad (11)$$

In this latter equation $1/\tau_c$ is the fluctuation rate of the magnetic field distribution, Δ . Physically these field fluctuations may arise from two different mechanisms: diffusion of the muon through the material or changes in direction and magnitude of Δ while the muon is localised. The latter is due to an electron spin relaxation process. The exponential damping can be measured in the transverse as well as the longitudinal mode. In the last mode one has a forward detector ($\theta = 0$):

$$N_F(t) = N_0 e^{-t/\tau_\mu} [1 + P(t) A] \quad (12)$$

and a backward detector ($\theta = 180^\circ$):

$$N_B(t) = N_0 e^{-t/\tau_\mu} [1 - P(t)A]. \quad (13)$$

The ratio

$$R(t) = \frac{N_F(t) - N_B(t)}{N_F(t) + N_B(t)} = AP(t) \quad (14)$$

gives directly the muon spin depolarisation function indexed according to the longitudinal direction of the applied field. Also zero field measurements are possible. In case of fast electron spin dynamics (no diffusion) above the magnetic ordering temperature, $P(t)$ is the same for transverse as longitudinal. The longitudinal measurement geometry is mostly used. It is possible to measure the damping rate over the range 0.001 and 100 MHz. The range of 5 decades is 3 decades wider than, for instance, in the case of Mössbauer spectroscopy.

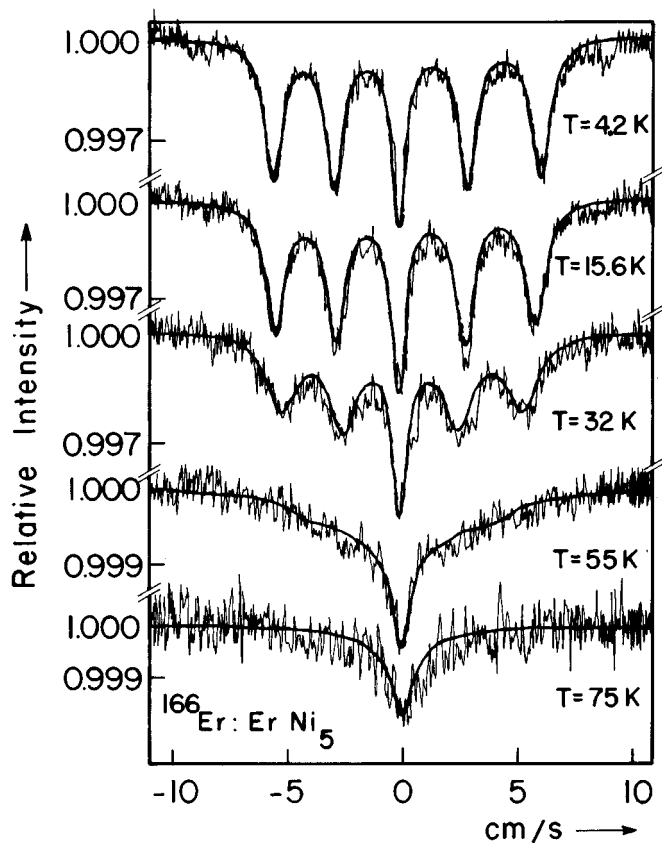


Fig. 1. ^{166}Er Mössbauer spectra of ErNi_5 . The curves are fits made with a spin up-spin down relaxation model.

From a technical point of view, μ^+ SR spectroscopy shows many similarities to PAC. However, the physical principle involved is related to the one of NMR. The advantage of μ^+ SR over NMR is the possibility to measure at zero field because

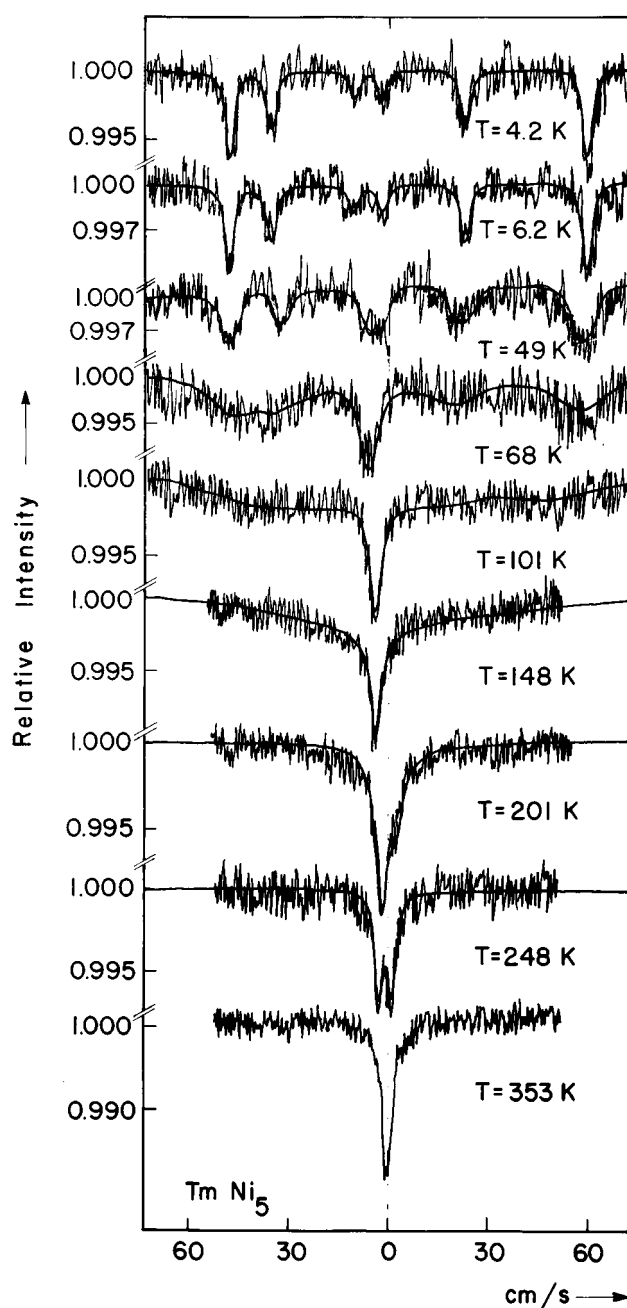


Fig. 2. ^{169}Tm Mössbauer spectra of TmNi_5 . The curves are fits made with a spin up–spin down relaxation model.

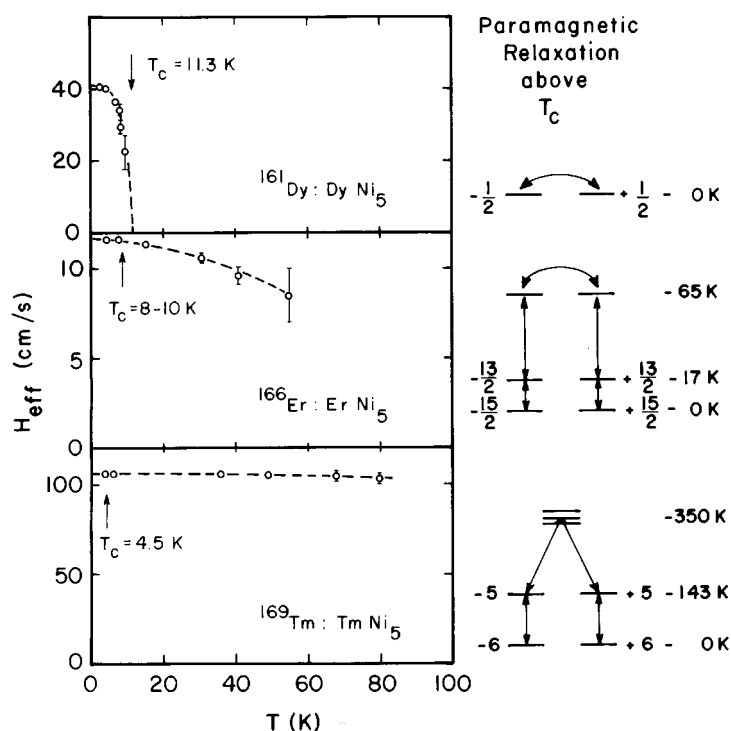


Fig. 3. Temperature dependence of the effective hyperfine field at the rare earth nuclei in DyNi_5 , ErNi_5 and TmNi_5 . The dashed lines are drawn to guide the eye. On the right the lower part of the corresponding crystal field diagrams are given. The double arrows indicate the nonzero transition probabilities.

the muon itself is polarised. In addition one does not need a particular nucleus as in the case of NMR, PAC and the Mössbauer effect. The muon can be implanted in every physical system. For a detailed analysis of the experimental data, the muon localisation site has to be determined. This can be done by changing the muon polarisation direction with respect to crystallographic directions. At higher temperatures the muon will diffuse (motional narrowing). Recent reviews of $\mu^+\text{SR}$ can be found in papers by Schenck and Gygax (1995) and Dalmas de Réotier and Yaouanc (1997).

The μSR measurements were performed at the ISIS facility of the Rutherford Appleton Laboratory in England and the Paul Scherrer Institute (PSI) in Switzerland.

5. Experimental Results and Discussion

(5a) ErNi_5 and TmNi_5

The RNi_5 compounds have the hexagonal CaCu_5 structure. The RNi_5 samples for Mössbauer spectroscopy were prepared by arc melting the 99.99%-pure starting materials in an atmosphere of purified argon gas. After annealing, the samples were examined by x-ray diffraction and found to be single phase.

Fig. 1 shows some of the ^{166}Er Mössbauer spectra of ErNi_5 measured between $T = 4.2$ and 75 K. The spectra measured below and above T_C show a clear five-line pattern. The Curie temperature determined for ErNi_5 equals $T_C = 9.1(2)$ K, measured by magnetic susceptibility. With increasing temperature the Mössbauer spectra show an increasing line broadening. This behaviour is typical for slow paramagnetic relaxation [see for instance Gubbens *et al.* (1985) and papers cited therein]. The spectra were analysed with a modified spin-up and spin-down model of Blume and Tjon (1968).

Fig. 2 shows the ^{169}Tm Mössbauer spectra of TmNi_5 measured between $T = 4.2$ and 353 K. The spectra measured just below and just above $T_C = 4.5$ K are identical and show a clear six-line pattern. With increasing temperature the spectra start to broaden, but remain magnetically split up to $T \sim 60$ K. Above this temperature the overall splitting decreases with increasing temperature. The spectra above $T = 100$ K show an asymmetric electric quadrupole doublet whose lines become of equal intensity at about $T = 250$ K. This behaviour is typical of a paramagnetic relaxation period, which is slower than the Larmor precession time. Since the quasi-doublet ground state is well isolated, these spectra can also be analysed with the spin-up and spin-down stochastic relaxation model of Blume and Tjon (1968).

In Fig. 3 we show the temperature dependence of the magnetic hyperfine field splitting of the ^{161}Dy , ^{166}Er and ^{169}Tm Mössbauer spectra of DyNi_5 , ErNi_5 and TmNi_5 , respectively. It can be seen that DyNi_5 orders magnetically below $T_C = 11.3$ K and shows no paramagnetic relaxation above this temperature, in contrast with the data shown for ErNi_5 and TmNi_5 in Fig. 3. We also show the lowest crystal field levels of the rare earth atoms in DyNi_5 , ErNi_5 and TmNi_5 . We take into account that transition probabilities are non-zero for magnetic and magnetoelastic transitions between crystal field levels with $\delta m_J = 0, \pm 1$ and ± 2 . As shown in Fig. 3 this means that in the case of DyNi_5 , which has an easy axis of magnetisation in the basal plane, a direct transition path exists between the two levels of the ground-state doublet, while in the cases of ErNi_5 and TmNi_5 only an indirect path is possible. In ErNi_5 there is a transition path between the states $|+\frac{15}{2}\rangle$ and $|-\frac{15}{2}\rangle$ via the excited state at an energy of 69 K, which is a doublet with the eigenfunctions $\mp 0.98|\mp\frac{11}{2}\rangle \pm 0.38|\pm\frac{1}{2}\rangle \pm 0.15|\pm\frac{13}{2}\rangle$. In TmNi_5 , however, a similar transition path can take place only for excitation energies of about 350 K. One may expect, therefore, that this kind of indirect transition path gives a longer relaxation time in TmNi_5 than in ErNi_5 . This agrees with the experimental observations. In TmNi_5 one observes relaxation effects up to about 250 K and in the case of ErNi_5 only up to 60 K. For an accurate determination of the corresponding relaxation times a fairly complex electronic relaxation model is required in the case of ErNi_5 .

Since for these RNi_5 compounds it is easy to grow single crystals, we have also studied them with μSR . The samples for μSR were prepared using the following method: a single crystal of about 1 cm^3 grown by the Czochralski technique is cut by spark erosion and the pieces are glued on a silver plate to give a mosaic of single crystals of about 8 cm^2 in area. We have used a TmNi_5 sample with the c axis perpendicular to the sample plane and two ErNi_5 samples, one with the c axis perpendicular to the sample plane and the other with the c axis in the sample plane. The samples were grown at the University of Amsterdam.

The measurements were performed both at ISIS and PSI over a temperature range of 0.2 to 340 K with a longitudinal experimental set-up and they were analysed using equation (12). With the PSI spin rotator, we were able to perform measurements with the initial muon beam polarisation either parallel or perpendicular to the c axis using only one sample. With this trick we have checked that the μ SR damping rate λ recorded on the two ErNi_5 samples is the same for identical experimental geometry. In Fig. 4 the ErNi_5 data are shown. When the muon beam polarisation is perpendicular to the c axis, the spectra are well described by a single exponential line, the asymmetry of which is temperature independent. Below $T \simeq 55$ K the damping rate is too large to be measured. We could not find any frequency below $T_C = 9.2$ K. When the muon beam is parallel to the c axis a single exponential function describes the data recorded above about 7 K. Below that temperature the signal is a sum of two components: an exponential and a time-independent function. Below 12 K we observed a drop of the total asymmetry by $\simeq 25\%$ compared to its high temperature value. Note that at this temperature $\lambda(T)$ has a maximum (see Fig. 4). This complicated temperature behaviour of the asymmetry indicates that the spin dynamics is quasi-static and/or the possibility of more than one muon site.

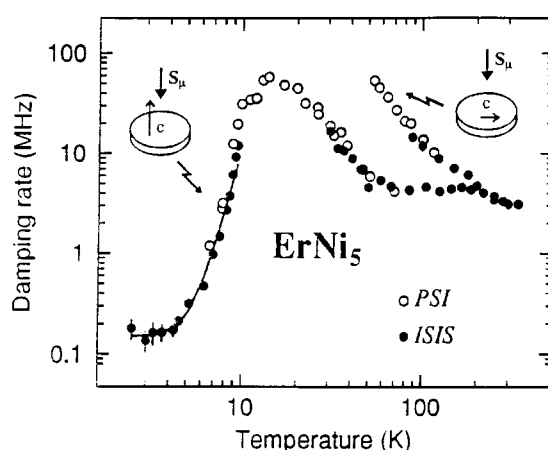


Fig. 4. Damping rate $\lambda(T)$ measured in zero field on ErNi_5 . The discrepancy between the data at low T is remarkably small despite the fact that they have been recorded at two different laboratories.

Fig. 4 shows that the damping is strongly anisotropic even at $T \sim 20 T_C$. Whereas λ starts to increase with decreasing temperature near 200 K when the polarisation is perpendicular to the c axis (designated as $\lambda = \lambda_{\perp}$), it keeps a constant value down to about 50 K, when the polarisation is parallel to the c axis (designated as $\lambda = \lambda_{\parallel}$). The λ_{\parallel} increase for $T < 50$ K is probably due to the fact that the magnetic fluctuations are quasi-static as indicated by the ^{166}Er Mössbauer spectroscopy measurements described earlier.

In an earlier publication (Gubbens *et al.* 1992a) we introduced a preliminary model for the high temperature ($T > 50$ K) behaviour of the relaxation rate. The

λ_{\perp} and λ_{\parallel} are first expressed in terms of the spin-spin correlation functions of the Er atoms. In our model the pair correlation functions have been neglected, which is justified at high temperature. The self-correlation functions are calculated in a high temperature approximation which ignores the Heisenberg interaction between the spins, when performing the thermal averages. Regarding the crystal field as an average two level system (spin up-spin down) we find that λ_{\perp} increases with decreasing temperature, while λ_{\parallel} is approximately constant, in agreement with the experimental results.

The data for $T < T_C$ can be understood using the following formula:

$$\lambda_{\parallel}(T) = a \coth(\Delta/k_B T) + bT^7, \quad (15)$$

where $a = 0.15$ MHz, $\Delta/k_B \geq 5$ K and $b = 1.1$ Hz K⁻⁷. This strong temperature dependence is a clear signal that the muon depolarisation is induced by the phonons.

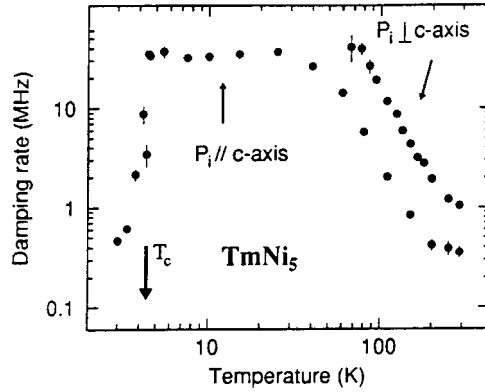


Fig. 5. Damping rate $\lambda(T)$ measured in zero field on TmNi₅.

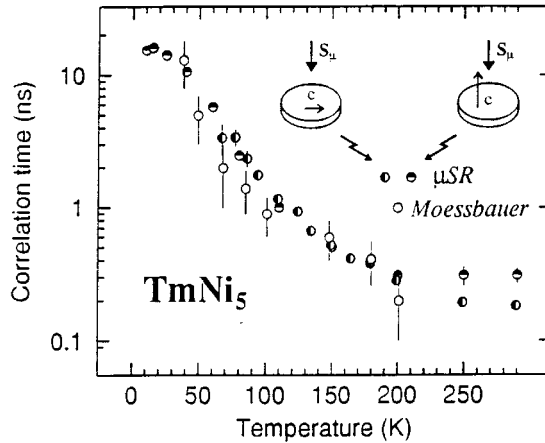


Fig. 6. Comparison between τ_c deduced from μ SR and ¹⁶⁹Tm Mössbauer data on TmNi₅.

As for the case of ErNi₅, zero field μ SR spectra for the single crystal of TmNi₅ were recorded at the PSI for the cases of initial muon polarisation parallel or perpendicular to the crystallographic c axis. With the spin rotator available at PSI, we have been able to measure both directions with the same sample. The corresponding damping rates, λ_{\parallel} and λ_{\perp} , are shown in Fig. 5 as a function of temperature. For the perpendicular geometry, the μ SR signal could not be detected below 67 K. However, for the parallel geometry, the signal was observable all the way down to 3 K. For this geometry, below the Curie temperature ($T_C = 4.5$ K), the damping rate is a measurement of the spin-lattice relaxation rate because the local field at the muon site is parallel to the c axis. As expected, the temperature behaviour of λ is qualitatively similar for ErNi₅ and TmNi₅.

We compare the high temperature behaviour of the observed relaxation rate in TmNi₅ with the one determined by ¹⁶⁹Tm Mössbauer spectroscopy using the following simple method. Because the depolarisation functions are described by exponential functions, we know that the data have been recorded in the ‘motional narrowing’ limit. Therefore we have $\lambda = 2\Delta^2\tau_c$, where Δ/γ_{μ} is the width of the field distribution at the muon site and τ_c the correlation time of the fluctuations. We have $\Delta^2 = c\langle J_z^2 \rangle$ where c is a temperature independent constant and J_z the projection of the total angular momentum of the rare earth ion along the c axis. Here $\langle J_z^2 \rangle$ can be computed from the known energy levels and eigenfunctions of the rare-earth ions. Therefore we can use the constant c as a scaling factor for comparison of τ_c deduced from ¹⁶⁹Tm Mössbauer spectroscopy with τ_c derived from the μ SR data as shown in Fig. 6. The close agreement between the temperature dependence of the two sets of correlation times supports our analysis of the μ SR data. We notice that the information deduced from the μ SR data is more precise. In addition, from these data it is possible to obtain information on the anisotropy of the fluctuations. This is impossible from the Mössbauer data because, by this technique, only the fluctuations along the easy axis can be measured. In conclusion we can state that ErNi₅ and TmNi₅ show a similar kind of magnetic behaviour. The ground state doublet of ErNi₅ (mainly $|\pm \frac{15}{2}\rangle$) and the quasi ground state doublet of TmNi₅ (mainly $|\pm 6\rangle$) show a similar kind of behaviour.

(5b) TmCu₂

The orthorhombic compounds DyCu₂, ErCu₂ and TmCu₂ (CeCu₂ structure) are antiferromagnetically ordered at $T_N = 26.7$, 11.5 and 6.3 K, respectively. The compounds DyCu₂ and ErCu₂ were studied with ¹⁶¹Dy and ¹⁶⁶Er Mössbauer spectroscopy (Gubbens *et al.* 1991). DyCu₂, which has a weak magnetic anisotropy with the a axis as the easy axis of magnetisation, shows no slow magnetic relaxation above T_N , just as in the case of DyNi₅. In contrast, ErCu₂ has a strong magnetic anisotropy parallel with the b axis as the easy axis of magnetisation and does exhibit slow magnetic relaxation behaviour above T_N . Both inelastic neutron scattering and Mössbauer effect measurements above T_N indicate that the Er atom in this compound has an isolated Kramers doublet as ground state, which consists mainly of the wave function $|\pm \frac{15}{2}\rangle$. As in the case of ErNi₅, ErCu₂ has an indirect relaxation path via excited doublet states at an energy of 72 K or higher.

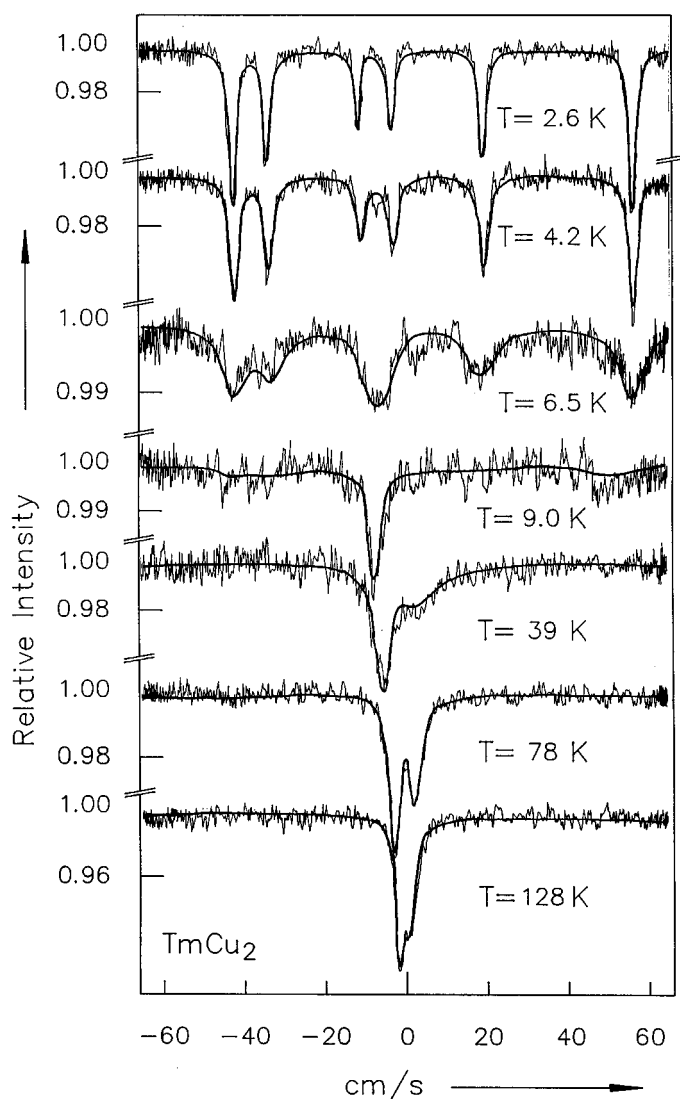


Fig. 7. ^{169}Tm Mössbauer spectra of TmCu_2 . The curves are fits made with a spin up–spin down relaxation model.

As in the case of ErCu_2 , TmCu_2 has a very strong magnetic anisotropy with the b axis as the axis of magnetisation. By combining the results of inelastic neutron scattering and ^{169}Tm Mössbauer spectroscopy an attempt was made to determine the nine crystal field terms for the Tm atom (Gubbens *et al.* 1992*b*). In Fig. 7 we show some representative ^{169}Tm Mössbauer spectra measured between $T = 2.6$ and 295 K. The spectra measured below $T_N = 6.3$ K show a clear six-line pattern. Above $T = 9$ K this pattern disappears and an asymmetric electric quadrupole doublet appears. The spectra were analysed with the same relaxation model as TmNi_5 .

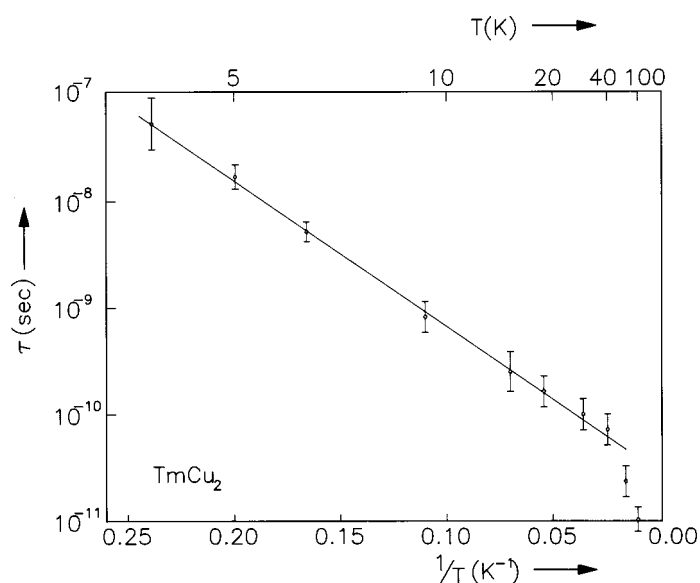


Fig. 8. Semi-logarithmic plot of the relaxation time τ against the inverse of the temperature. The line represents an exponential law.

From the combined analysis of the inelastic neutron scattering measurements and the temperature dependence of the electric quadrupole splitting we found the lowest two crystal field levels of Tm to be as shown in equations (4) and (5). The eigenfunctions are only slightly mixed. Therefore, the 4f contribution of the electric quadrupole splitting has almost the free ion value. The splitting between the two levels of the isolated quasi-doublet ground state equals 1.0 K. In Fig. 8 the calculated relaxation times τ_c for TmCu₂ have been plotted semi-logarithmically against the inverse temperature. The behaviour of the relaxation time is proportional to an exponential law of the inverse temperature. This behaviour is the same as in the case of ErNi₅ and TmNi₅. Effectively, the eigenfunctions form an almost pure $|\pm 6\rangle$ quasi-doublet ground state. This kind of problem has also been encountered above in TmNi₅.

(5c) TmCuAl

The ternary compound TmCuAl has the hexagonal Fe₂P structure with Cu on the phosphorus site and Tm and Al on the two inequivalent iron sites. Specific heat, magnetic susceptibility and electrical resistivity measurements show that TmCuAl orders antiferromagnetically at about 1.9(1) K (Gubbens *et al.* 1998). Since the *c* axis of ErCuAl is the easy magnetisation axis (Javorsky *et al.* 1997), it can be expected that TmCuAl has also axial magnetic anisotropy. In this section we will show the results of a ¹⁶⁹Tm Mössbauer spectroscopy study.

The Tm site has orthorhombic local symmetry. All even terms must be included in the crystal field Hamiltonian so that the two lowest levels are mixed as described in Section 2.

In Fig. 9 we show ¹⁶⁹Tm Mössbauer spectra of TmCuAl measured above $T_N = 1.9$ K. The spectra consist of an asymmetric electric quadrupole doublet

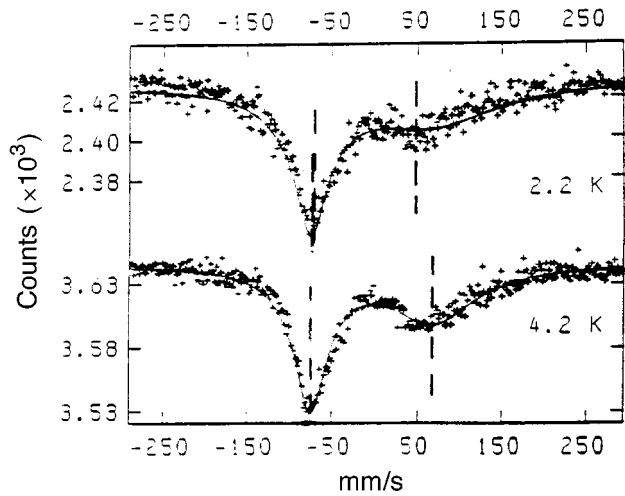


Fig. 9. ^{169}Tm Mössbauer spectra of TmCuAl measured at $T = 2.2$ and 4.2 K. The curves are calculated with a spin up–spin down relaxation model. The peak positions related to the pseudo quadrupole shift are indicated.

typical for magnetic relaxation. Moreover, below 10 K, it is observed that the centre of this quadrupole split doublet shifts increasingly towards negative velocity as the temperature decreased, despite the fact that ^{169}Tm Mössbauer spectra are not subject to an isomer shift. This effect is due to a second order perturbation effect such as first explained by the pseudo-quadrupole interaction theory of Clauser *et al.* (1966). Usually, one observes two lines, of which the right one is more relaxation broadened than the left one. As the temperature is decreased the right-hand line is more shifted to the left than the left peak to the right as shown in Fig. 9 for TmCuAl . Therefore, this behaviour enables us to determine the energy difference between the two crystal field levels of the quasi ground state doublet in TmCuAl by using the formula:

$$E(T) = E(T = 0) \tanh(\Delta/2T), \quad (16)$$

where $E(T)$ is the shift of the centre of gravity, the so-called pseudo-quadrupole shift, and Δ is the distance between the two crystal field levels as shown by Clauser *et al.* (1966). In Fig. 10 we show the temperature dependence of the pseudo-quadrupolar shift. Using formula (16), we determined that the distance between the two levels of the quasi-doublet is 2.8 ± 0.3 K.

The ^{169}Tm Mössbauer spectrum recorded recently for TmCuAl at $T = 0.32$ K (well below $T_N = 1.9$ K) is a superposition of a quadrupole-split doublet and a magnetically-split sextet. The same type of composite spectrum was recorded at $T = 1.1$ K when the temperature had been raised from 0.32 K. However, when the temperature was decreased to 1.1 K from 4.2 K a pure quadrupole-split doublet spectrum was observed. This temperature hysteresis indicates that the magnetic transition is first order. The electric quadrupole splitting at $T = 3.3$ K is $14.9(1)$ cm/s. This value is slightly smaller than can be expected on basis of

the crystal field due to the influence of the pseudo-quadrupole behaviour. The deviation from the free ion value of 15.7 cm/s for ^{169}Tm is rather small. This indicates that the main contribution to the eigenfunctions of the two lowest levels is indeed $|\pm 6\rangle$ as shown in formulas (4) and (5) and that mixing of pure angular states is limited.

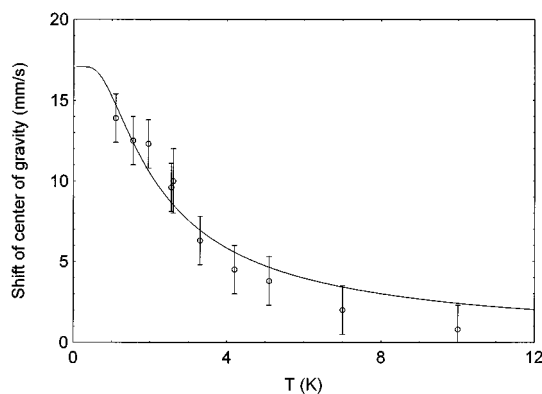


Fig. 10. Temperature dependence of the shift of gravity of the electric quadrupole splitting of TmCuAl. The curve is a fit with equation (16) and corresponds to an energy separation of 2.8 ± 0.3 K for the two levels of the quasi-doublet ground state.

The spectra were simulated using a stochastic theory to determine the magnetic relaxation times (solid curves in Fig. 9). The relaxation times determined are proportional to the inverse of the temperature as shown in Fig. 11. This result is characteristic of a direct relaxation process between the two energy levels.

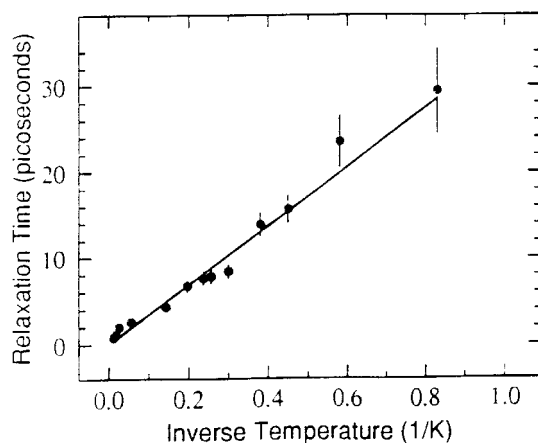


Fig. 11. Inverse temperature dependence of the relaxation times determined for Tm-CuAl.

In conclusion we remark that the pseudoquadrupole shift of ^{169}Tm Mössbauer spectroscopy gives a unique possibility to study the relaxation behaviour between the two low-lying levels with eigenfunctions mentioned in formulas (4) and (5).

Neutron techniques fail in this case. However, a very low magnetic ordering temperature, a magnetic c axis anisotropy and an energy splitting between the two levels of only a few kelvin are necessary for observing the ^{169}Tm pseudo-quadrupole shift.

(5d) PrRu_2Si_2

The compound PrRu_2Si_2 has the tetragonal ThCr_2Si_2 structure. The following measurements have been performed on polycrystalline samples, except for the magnetisation and muon spin relaxation measurements which were carried out on single crystals. For an extended description of the measurements and the analysis of the results we refer to Mulders *et al.* (1997). In this paper we shall give only a summary of the scientific results and their explanation.

The temperature dependence of the magnetic specific heat of PrRu_2Si_2 , measured at temperatures ranging from 4.3 to 67 K, is presented in Fig. 12. The lattice and conduction electron contributions have been estimated from measurements on LaRu_2Si_2 and are subtracted from the raw PrRu_2Si_2 data. A well-defined anomaly is observed at the ferromagnetic ordering temperature $T_C = 14.0$ K. In addition a weak anomaly is observed starting at ~ 16 K (see the inset of Fig. 12). As we will show later in this section this anomaly corresponds to a second magnetic phase transition.

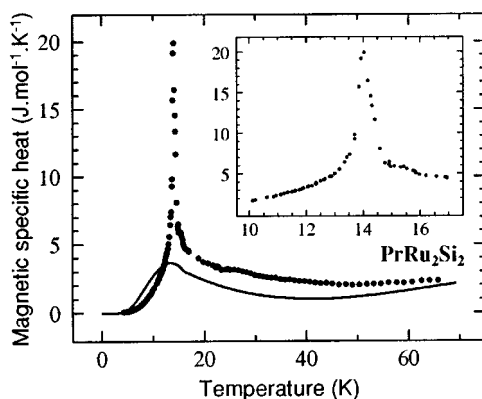


Fig. 12. Temperature dependence of the magnetic specific heat of PrRu_2Si_2 . The lattice and conduction electron contribution has been estimated from measurements on LaRu_2Si_2 and subtracted from the raw PrRu_2Si_2 data. The solid curve is the prediction of the molecular field approximation with the energy levels shown in Fig. 17. The contribution of the two phase transitions is not taken into account.

The magnetisation measurements were performed using a SQUID magnetometer. They indicate that the bulk magnetic moment at 4.5 K is $2.69 \mu_B$ per Pr atom. We notice that even at a temperature twice the value of T_C the magnetic anisotropy is strong: whereas in an applied magnetic field of 5.5 T the magnetisation at 28 K is $2.5 \mu_B$ per Pr atom when measured along the c axis, it is only $0.032 \mu_B$ per Pr atom for the field applied along the a axis. High field magnetisation

measurements have been performed in fields up to 35 T. These measurements confirm the strong magnetic anisotropy of this compound. At 4.2 K, in an applied field of 35 T, the value of the magnetisation measured along the c and a axes is $3.08 \mu_B$ and $0.39 \mu_B$, respectively.

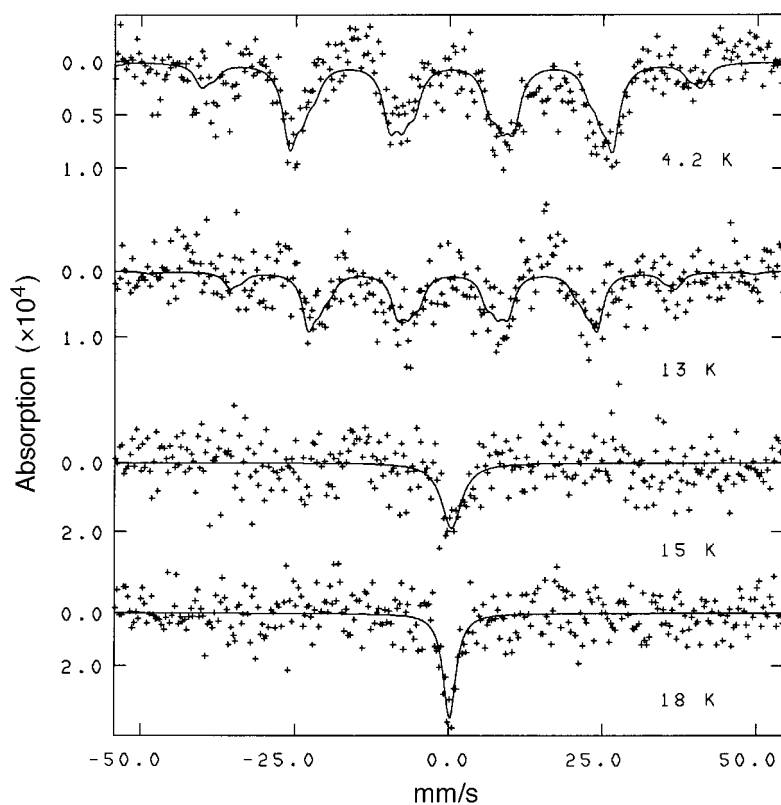


Fig. 13. Representative ^{141}Pr Mössbauer spectra of PrRu_2Si_2 . The curves represent fits with the isomer shift and the magnetic hyperfine field as free parameters. From the hyperfine field fitted at 4.2 K the Pr $4f$ moment is deduced to be $2.76 \mu_B$.

The ^{141}Pr Mössbauer spectra were recorded at temperatures from 4.2 to 25 K. Some of the spectra measured are shown in Fig. 13. No slow relaxation behaviour is found above $T_N = 16.0(1)$ K. From the splitting of the absorption lines, a hyperfine field at the nuclear site of $281(2)$ T is deduced. This corresponds to a Pr $4f$ magnetic moment of $2.76 \mu_B$. The small difference between this value and the value measured by magnetisation is understood if we remember that the $5d$ electrons of any rare-earth ion contribute to the bulk magnetisation. This $5d$ moment equals $\sim 0.1 \mu_B$ and is oriented antiparallel to the $4f$ moment for a light rare-earth ion.

μSR experiments have been carried out at the ISIS surface muon facility. Fig. 14 shows $\lambda(T)$ recorded in an applied longitudinal field of 0.2 T. This field is necessary to suppress the depolarisation due to the ^{141}Pr nuclear magnetic moments, the effect of which is enhanced by the large hyperfine coupling constant

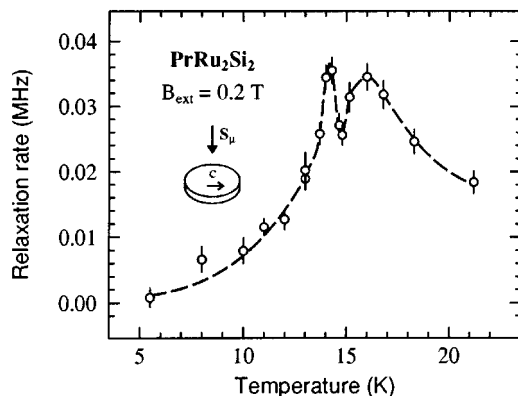


Fig. 14. Temperature dependence of the μ SR longitudinal exponential damping rate measured on PrRu_2Si_2 with $B_{ext} = 0.2$ T. The initial muon polarisation is perpendicular to the c axis. The critical temperatures of the two magnetic phase transitions are located at temperatures, for which the relaxation rate exhibits maxima. The dashed curve is a guide to the eye.

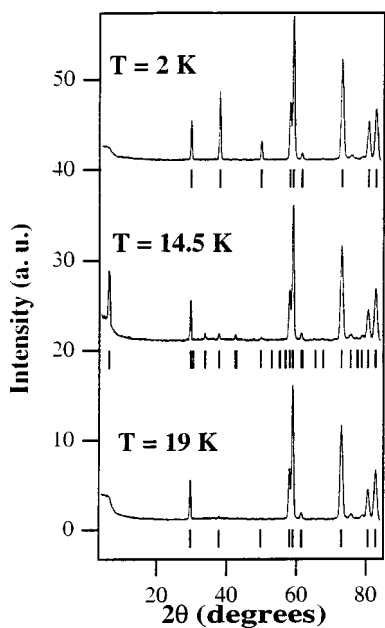


Fig. 15. Neutron powder diffraction patterns from paramagnetic ($T = 19$ K), incommensurate plus ferromagnetic ($T = 14.5$ K) and ferromagnetic ($T = 2$ K) phases of PrRu_2Si_2 .

and Van Vleck susceptibility. The function $\lambda(T)$ presents two maxima, one at ~ 14 K and a second one at ~ 16 K. This shows that, in addition to the phase transition at T_C , there is a second magnetic phase transition at $T_N \sim 16$ K. Although it is difficult to detect T_N in the magnetic specific heat data, muon spectroscopy clearly shows its signature.

In order to further study the transition at T_N , we have performed neutron powder diffraction measurements in the temperature range 2–19 K. These experiments have been carried out in Grenoble at the Siloé reactor of the Commissariat à l’Energie Atomique on the DN5 linear multidetector diffractometer using an incident neutron wavelength of 2.487 Å.

Between $T_N \sim 16.0$ K and $T_C \sim 14.0$ K, additional reflections can be identified as shown in Fig. 15. The new reflections, due to the onset of the magnetic order, can be indexed with a wave vector $\tau = (0.133, 0.133, 0)$ which is temperature independent. The magnetic moments of this sine wave modulated structure are parallel to the c axis with an amplitude of 1.8 (1) μ_B per Pr atom at 14.5 K. Besides these reflections, additional intensities appear on the nuclear Bragg reflections that can be accounted for by a ferromagnetic contribution with the magnetic moments along the c axis. At 14.5 K the ferromagnetic moment is 1.0 (1) μ_B per Pr atom. The ratio of the intensities of the two magnetic components depends on the experimental procedure, i.e. spectra recorded in cooling down or in warming up the sample. This is a characteristic for a first order transition at T_C .

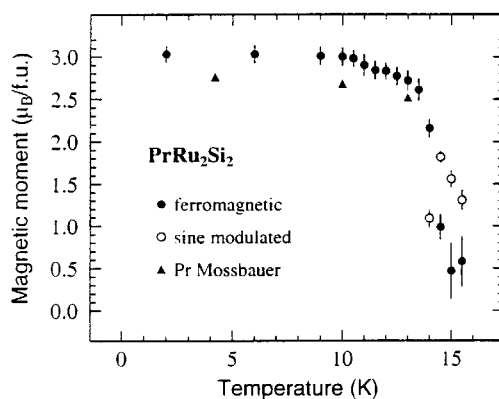


Fig. 16. Temperature dependence of the $4f$ magnetic moment measured by neutron diffraction in PrRu_2Si_2 . Below 14 K an axial ferromagnetic structure is observed (filled circles). Between 14 and 16 K a second magnetic structure is observed characterised by an incommensurate sine wave modulation with $\tau = (0.133, 0.133, 0)$ (empty circles). In addition the $4f$ magnetic moment measured at three temperatures by $^{141}\text{Mössbauer}$ spectroscopy is presented (filled triangles). Both data sets show that the ferromagnetic transition at 14 K is first order.

Below T_C the sine wave phase has disappeared and only the ferromagnetic contribution remains with a Pr $4f$ moment of 3.0 (1) μ_B at 2 K. Although this value is slightly larger than the one deduced from magnetisation and Mössbauer measurements ($\sim 2.8 \mu_B$), it is still reasonable taking into account the difficulty in measuring precisely the intensity of the Bragg peaks in a textured powder sample. The results of these measurements are shown in Fig. 16.

The inelastic neutron scattering (INS) method has been used to extract information on the energy level scheme of PrRu_2Si_2 . In order to simplify the analysis of the INS data the measurements are performed only in the paramagnetic phase. Since our specific heat measurements indicate that a crystal field energy

level is located at low energy, we have carried out the measurements on a sample with the Pr ions partly substituted by non-magnetic La ions. The substitution is expected to depress the magnetic ordering temperature but not to drastically modify the crystal field acting on the Pr ions. We have chosen $\text{La}_{0.5}\text{Pr}_{0.5}\text{Ru}_2\text{Si}_2$ because magnetisation measurements show that it is still paramagnetic at 2 K.

The INS measurements have been performed in Grenoble with the DN6 time-of-flight spectrometer located at the Siloé reactor. In the energy range 1–40 meV we have detected only two inelastic peaks corresponding to crystal field excitations at 2.25 (5) meV and 28.4 (1) meV. The large magnetic moment observed at low temperature in combination with the specific heat and INS data allows us to specify the nature and location of some of the crystal field levels.

We first notice that at $T \ll T_C$ the magnetic moment is so large that the crystal field ground state must contain the $|\pm 4\rangle$ states. Here $|\Gamma_{t1}^{(1)}\rangle$ is the ground state of \mathcal{H}_C because it has the lowest energy. This state is a non-magnetic singlet. It is known that a large magnetic moment can be generated at low temperature from a magnetic singlet only if there is at least one crystal field energy level located at an energy comparable to the exchange energy. Since PrRu_2Si_2 is an axial ferromagnet, the exchange field is proportional to a J_z matrix element. Therefore the first excited crystal field state, must be such that $\langle J_z \rangle$ is non-zero. The only possible first excited state is $|\Gamma_{t2}\rangle$ since the $|\Gamma_{t1}^{(2)}\rangle$ state is located at higher energy. The location of this energy is at $\Delta = 2.25$ (5) meV. The only other possible neutron transitions from the ground state are to the $|\Gamma_{t5}^{(1)}\rangle$ and $|\Gamma_{t5}^{(2)}\rangle$ states (see Mulders *et al.* 1997). The $|\Gamma_{t5}^{(1)}\rangle$ state being the lowest in energy, we attribute the peak observed at 28.4 (1) meV to the transition from the ground state to this state. We infer a substantial value for $\sin^2 \beta_2$, which is most likely approximately 1. In Fig. 17 we show the four lowest lying crystal field levels.

In summary, the crystal field ground state and first excitation state are singlet states well separated in energy from the other crystal field states. Therefore the low temperature magnetic properties of PrRu_2Si_2 should be understood by considering the Pr^{3+} ions as two-level systems interacting on a lattice. It was recognised a long time ago that exchange interactions induce magnetic ordering in a singlet crystal field ground state if these magnetic interactions are strong enough. An expression for the magnetisation of the $4f$ electrons at $T = 0$ is obtained in the molecular field approximation (Bleaney *et al.* 1963):

$$M_{4f}(T = 0) = 4g_J\mu_B \sin \beta_1 \left[1 - \tanh^2 \left(\frac{\Delta}{2k_B T_C} \right) \right]^{\frac{1}{2}}, \quad (17)$$

where g_J is the Landé factor ($g_J = \frac{4}{5}$ for Pr^{3+}), μ_B the Bohr magneton, k_B the Boltzmann constant and $\Delta = E_{t2} - E_{t1}^{(1)}$. Our measurements give $\Delta = 2.25$ meV and $T_C = 14$ K. The observed INS peak intensity as well as the size of the magnetic moment indicate a value of $\sin^2 \beta_1$ close to 1. Using $\sin \beta_1 = 1$ and equation (17) we deduce that the maximum value of $M_{4f}(T = 0)$ is $2.18 \mu_B$ per Pr atom. This is much lower than the experimental value of $2.8 \mu_B$.

To explain the observed moment value within the molecular field approximation, Δ should be reduced substantially or the magnetic ordering temperature should

be drastically raised, i.e. we should have $\Delta/2k_B T_C = 0.53$ instead of 0.93. The first possibility is excluded since an INS transition is clearly observed at 2.25 meV and also the entropy shows no sign of a singlet below ~ 20 K. The second possibility is also excluded since specific heat, μ SR and neutron diffraction indicate magnetic transitions at 14 and 16 K.

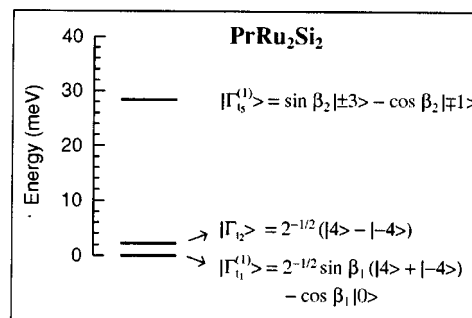


Fig. 17. Crystal electric field energy level scheme of the Pr^{3+} ions in PrRu_2Si_2 deduced in this work. The inelastic neutron investigation did not detect any other states below 40 meV. The five states not mentioned in the figure are most likely located above 40 meV. They do not influence the magnetic properties at low temperature. The β_1 and β_2 values are near $\pi/2$.

In addition, the shape of the magnetisation curve as presented in Fig. 16 is more rectangular than a Brillouin curve. This is a signature of a first order transition. In contrast to this, the molecular field approximation predicts that the ferromagnetic transition is second order (see Fig. 18).

Although the molecular field approximation does not provide a reasonable description of the measurements, it should be useful to understand the specific heat data since they should be dominated by the effect of the crystal field levels, i.e. by the Schottky anomaly. We do not attempt to describe the specific heat related to the magnetic phase transitions. The solid curve in Fig. 12 represents the calculated specific heat with a singlet at $E_{t2} = 2.25$ meV and a doublet at $E_{t5}^{(1)} = 28.4$ meV. Below T_C the effect of the molecular field is taken into account. The discrepancy between the model and the experimental data is small.

We have showed that the molecular field approximation fails to provide a good description of the magnetic moments. Since the two singlets are close together, collective excitations of the singlet ground state take place (Wang and Cooper 1969). These excitations are passed on from one atom to another, a process similar to that observed in spin waves. The most simple theory which attempts to account for these excitations is the random phase approximation (RPA). In the paramagnetic state its Hamiltonian reduces to the Ising Hamiltonian in a transverse field. The energy spectrum of the excitations shows dispersion with a minimum energy gap at $\mathbf{k} = 0$ (zone centre). The shape of the dispersion and the size of the energy gap depend on the exchange strength and the relative temperature $k_B T/\Delta$. Reaching T_C from either above or below, the energy gap decreases towards zero. This reduction of the energy gap is an effective channel

to depopulate the singlet ground state and therefore, in the RPA, T_C is reduced compared with the molecular field approximation. Also the RPA magnetisation curve is more rectangular due to this effect and the transition to the paramagnetic state becomes first order. In Fig. 18 we present its predictions using the formalism of Wang and Cooper (1969). It provides a better description than the molecular field approximation: it predicts that the transition is first order and yields a larger moment at low temperature. But this moment is still $\sim 15\%$ smaller than observed.

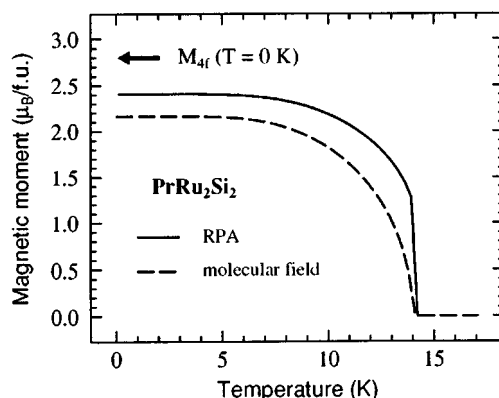


Fig. 18. Calculated magnetisation curve in the molecular field approximation (dashed curve) and the random phase approximation (solid curve). The arrow indicates the value of the magnetic moment of the $4f$ electrons as deduced from magnetisation and Mössbauer measurements.

In conclusion our study has shown that the RPA gives a better description of the low temperature properties of PrRu_2Si_2 than the molecular field approximation. We note that $k_B T_C$ is of the same order as Δ and strong correlations effects are hence expected. However, these effects are not sufficiently taken into account in the RPA. Since the crystal field parameters of PrRu_2Si_2 are now well defined, this compound provides a good system to test theoretical predictions for these correlation effects. In addition, inelastic neutron scattering experiments on single crystals could reveal the nature of the dispersion.

6. Conclusions

In this review we have compared four intermetallic compounds of Tm and Pr, exhibiting a range of energy separations for the quasi-doublet ground-state level of the rare earth ions. It appears that with an increasing separation between the two energy levels the magnetic dynamic behaviour changes dramatically. Firstly, TmNi_5 , for which the energy separation 0.4 K, has the same magnetic dynamic behaviour as the Kramers doublet compound ErNi_5 , μSR and Mössbauer measurements show a long indirect relaxation path above T_C , for which the temperature dependence of the magnetic fluctuations has an exponential character. Moreover, from the Mössbauer effect it appears that in TmNi_5 the eigenfunctions of the two levels of the ground-state doublet are almost pure in $|\pm 6\rangle$ as given

in equations (4) and (5). TmCu_2 has the same behaviour as TmNi_5 . The magnetic relaxation path is much shorter in time, probably due to the larger energy separation of the two levels of the ground-state doublet (1.0 K). Both compounds TmNi_5 and TmCu_2 have a second order transition.

In contrast, TmCuAl behaves quite differently. The distance between the two crystal field levels of the ground-state doublet is 2.8 K. The magnetic relaxation above T_N shows a $1/T$ behaviour, which means a direct relaxation between the two levels. Moreover, the magnetic transition shows a clear first order transition. It appears that the pseudo-quadrupolar shift is a very nice tool to determine the distance of the two energy levels of the quasi-doublet.

Finally, ^{141}Pr Mössbauer measurements show no magnetic relaxation above T_N . The energy separation of the two levels of the quasi-doublet amounts to 25 K. Although this is quite large, magnetic ordering exists up to 16 K. The random approximation model we used to explain the results also explains the first order transition behaviour.

Acknowledgments

The authors would like to thank the Dutch Scientific Organisation (NWO) for support. They also wish to thank those people who have contributed very much to the research which is discussed in this overview. Firstly, the significant contributions of A. Yaouanc and P. Dalmas de Réotier of CEA Grenoble to the paragraphs concerning the μSR and neutron work on RNi_5 and PrRu_2Si_2 were essential. Furthermore, the production of single crystals of RNi_5 and PrRu_2Si_2 at the van der Waals–Zeeman Laboratory in Amsterdam must be acknowledged. M. Divis of the Charles University in Prague contributed significantly to the interpretation of the results for the RCu_2 compounds. The help of R. van Geemert was substantial for the interpretation of the TmCuAl results. Finally, it is necessary to acknowledge the overall support of K. H. J. Buschow for this type of research.

References

- Bleaney, B., *et al.* (1963). *Proc. R. Soc. London A* **276**, 19.
- Blume, M., and Tjon, J. A. (1968). *Phys. Rev.* **165**, 446.
- Clauser, M. J., *et al.* (1966). *Phys. Rev. Lett.* **17**, 5.
- Dalmas de Réotier, P., and Yaouanc, A. (1997). *J. Phys. C* **9**, 9113.
- Gubbens, P. C. M., *et al.* (1985). *J. Magn. Magn. Mater.* **50**, 199.
- Gubbens, P. C. M., *et al.* (1989). *Phys. Rev. B* **39**, 12548.
- Gubbens, P. C. M., *et al.* (1991). *J. Magn. Magn. Mater.* **98**, 141.
- Gubbens, P. C. M., *et al.* (1992a). *J. Magn. Magn. Mater.* **104–7**, 1269.
- Gubbens, P. C. M., *et al.* (1992b). *J. Magn. Magn. Mater.* **104–7**, 1283.
- Gubbens, P. C. M., *et al.* (1995). *Hyperfine Int.* **85**, 239.
- Gubbens, P. C. M., *et al.* (1998). *J. Magn. Magn. Mater.*, accepted for publication.
- Javorsky, P., *et al.* (1997). *Physica B* **225**, 230.
- Kayzel, F. E. (1997). Thesis, University of Amsterdam.
- Mulders, A. M., *et al.* (1997). *Phys. Rev. B* **56**, 8752.
- Schenck, A., and Gygax, F. (1995). In 'Handbook of Magnetic Materials', Vol. 9 (Ed. K. H. J. Buschow), pp. 57–302 (Elsevier: Amsterdam).
- Wang, W. L., and Cooper, B. R. (1969). *Phys. Rev.* **185**, 696.